JOURNAL OF MATERIALS SCIENCE **35** (2000) 1269–1281

Surface topography and wear mechanisms in polyamide 66 and its composites

Y. K. CHEN*
The University of Hertfordshire, Materials Group, Department of Aerospace, Civil and Mechanical Engineering, Hatfield, Herts AL10 9AB, UK
E-mail: y.k.chen@herts.ac.uk

S. N. KUKUREKA
The University of Birmingham, School of Metallurgy and Materials, Edgbaston, Birmingham, B15 2TT, UK

C. J. HOOKE, M. RAO
The University of Birmingham, School of Manufacturing and Mechanical Engineering, Edgbaston, Birmingham, B15 2TT, UK

A study has been made of the tribological behaviour of polyamide 66 (PA66) running against itself, in unlubricated, non-conformal and rolling-sliding contact. Tests were conducted over a wide range of loads and slip ratios using a twin-disc test rig. The wear and friction behaviour of unreinforced PA66 is dominated mainly by three major features: a critical slip ratio under a fixed load and running speed, macro-transverse cracks and a layer of film on the contact surface. Both the wear and friction properties of unreinforced PA66 can be improved considerably by filling with 20wt% PTFE, and the tribological mechanisms are changed significantly. This reinforcement prevents both the initiation and propagation of transverse cracks on the contact surfaces which occurred in the unreinforced material. It also decreases both the wear rate and the friction coefficient substantially. The 30wt% short glass-fibre reinforced PA66 also suppresses the transverse cracks from initiation on the surfaces. A thin film on the contact surfaces plays a dominant role in reducing wear and friction of the composite and in suppressing the transverse cracks. These results offer the prospect of enhanced applicability of PA66 in engineering components.

1. Introduction

Polymers and polymer composites as gear materials represent an interesting development for gearing because they offer high strength-to-weight ratio, ease of manufacture and excellent tribological properties [1–5]. In particular, there is a sound prospect that polymer composite gears can be applied for not only motion but power transmission of up to 10 kW [6, 7]. A number of national and commercial standards do exist for the design and rating of polymer gears [8, 9] but they have been adapted from design standards for metal gears [10] with little modification. Some types of failure modes of PA66 gears, such as frequent fractures in bending near the pitch point rather than at the dedendum [7, 11, 12], have not been represented in any of the standards. A number of studies of PA66 gear behaviour have been made [6, 12] but these have been mainly associated with running PA gears against metal gears and failure mechanisms of PA gears running against steel gears are clearly different from those of PA gears running against PA gears [6, 7, 11, 12]. Therefore, the failure mechanisms of polyamide 66 (PA66) gears when they run against themselves are still not clear although in engineering polymer gears running against polymer gears are more common than using polymer against metals. As a result, PA66 users have to substantially under-rate their designs for gears. The difficulty of interpreting the results from the performance of PA66 gear to establish the effects of reinforcement on their wear and friction behaviour necessitated a comprehensive study of these materials.

This present work was thus initiated to study wear and friction mechanisms and the surface topography of unreinforced PA66 and its composites. It was hoped that this investigation would enable the failure mechanisms of PA66 gears and other non-conformal engineering components to be interpreted. The materials were tested running against themselves, in unlubricated, non-conformal and rolling-sliding contact in order to correspond to the conditions used for gears [13–17]. Tests were conducted over a wide range of loads and slip ratios using a twin-disc test rig [14–16]. In the present

* Author to whom all correspondence should be addressed.

paper, the unique wear and friction behaviour of the ordinary unreinforced PA66 is outlined: a critical slip ratio under a fixed load and running speed, macro-transverse cracks and a layer of film on the contact surface. The tribological properties of unreinforced PA66 can be improved considerably by filling either with 20wt% PTFE or 30wt% short glass-fibres, and as a result, both the wear mechanisms and surface topography are changed significantly. Both the reinforcement of glass fibre and the filler of PTFE prevent both the initiation and propagation of transverse cracks on the contact surfaces which occurred in the unreinforced material and suppress the appearance of a critical slip ratio which appears with unreinforced PA66. It also decreases both the wear rate and the friction coefficient substantially. The results of this paper offer the prospect of enhanced applicability of PA66 in gearing.

2. Experimental details

The twin-disc wear testing machine used in our previous work [14–16, 18] was again employed in this investigation. With this machine, measurements of both the frictional force and wear (as a change in radius) between two discs in contact can be made continuously so that both the wear process and friction behaviour during tests can be monitored. Wear was also measured by weighing the discs before and after a test. Experiments were carried out either at different slip ratios under a given normal load or at different loads with a given slip ratio. With this method the typical loading and sliding conditions of engineering components in non-conformal, rolling-sliding contact can be simulated [14–17].

The materials used were supplied by LNP Ltd. and were polyamide 66 (R1000), 20wt% PTFE filled PA66 (RL4040) and short-glass fibre reinforced PA66 (RF1006 HS) [3]. The proportions of glass fibre added was 30 wt%. To ensure proper contact along the facewidth of the discs all of the specimens were prepared by machining 20 μm from the moulded surface and then polishing to a surface roughness of around 5 μm. Both the discs were 30 mm in diameter and 10 mm in facewidth.

Before testing, the disc samples were cleaned with methanol. They were then run at the test conditions for an extended period to bed-in the surfaces and to remove the machining asperities and any subsurface layer affected by the manufacturing process. After bedding-in they were dried at 70°C for 15 hours to remove any absorbed water that might affect the measurement of wear and then weighed. Finally, they were left under atmospheric conditions for about two weeks to allow the water content to return to equilibrium conditions. After this preliminary treatment the specimens were remounted in the test rig in an identical position to that under which they had been run-in.

Tests were run for running speed of 1000 rpm (the rotational speed of the lower disc [14–16]) and at a range of loads and slip ratios. Slip ratio is defined here as the ratio of sliding to rolling velocities. If the tangential velocities on both contact surfaces are v_1 and v_2 respectively then the sliding velocity is $(v_1 - v_2)$ and the rolling velocity is $(v_1 + v_2)/2$. The slip ratios used were between 0 and 0.28. Tests were operated under dry, unlubricated conditions at ambient temperature $(22 \pm 1)^\circ$C until failure or for up to 10^7 contact cycles.

At the end of the test the discs were again dried at the same temperature and for the same time period as those before they were tested. Then, the discs were weighed to measure the weight loss of each disc. With this drying procedure the measurement of wear by weighing is accurate to about $\pm 10^{-5}$g. Without drying the accuracy appeared to be limited to $\pm 10^{-3}$g. Finally, the worn surfaces were observed in detail by using a JEOL JSM6300 Scanning Electron Microscope.

3. Experimental results

3.1. Wear and friction behaviour of unreinforced PA66

Typical results of wear versus number of contact cycles are shown in Fig. 1. These are for a running speed of 1000 rpm and a normal load of 200 N. The wear shown in Fig. 1 was monitored with a real-time data-logging system and was measured as the separation of the disc centres while material on the disc surfaces is being removed during the tests [14–16]. A number of phenomena can be seen: For the group of slip ratios between 0.09 and 0.11, as shown in Fig. 1a, it appears that the wear can be divided into three phases: viz the period where temperature increases, a nearly linear wear region and steep linear wear period. In the first period, because the temperature was rising, thermal expansion of the specimens occurred and resulted in an increase of the central distance between the discs so that a "negative wear" was measured. This period was rapidly replaced by the second one—the nearly linear wear period. During this progressive and approximately linear wear stage which corresponds to a higher friction coefficient of between 0.62 and 0.72, much wear debris was noticed and it appeared flake-like at 0.09 slip ratio and as fibrils like cotton at 0.11 slip ratio.

Fig. 1b shows that as for the group of slip ratios between 0.14 and 0.21, the wear can also be divided into three phases: a region where surface temperature rises, a steep linear wear period which precedes a subsequent period of less steep linear wear. Unlike in Fig. 1a, the gradient of this third period at these slip ratios is much smaller. This third period corresponds to a low friction coefficient of 0.28 at a slip ratio of 0.21 and a friction coefficient of 0.43 at a slip ratio of 0.14. It was noted that during the tests in this third period, samples ran very smoothly and the surfaces of the samples became more polished and discoloured. Also, not very much wear debris was noticeable in this period.

As for a slip ratio of 0.04, as shown in Fig. 1c, only two phases of the wear curve can be found. It was noted that during the tests in this second period, samples ran very smoothly and the surface behaviour observed during the test was similar to that at a high slip ratio of 0.21 as shown in Fig. 1b. The surface here also became dark brown and discoloured. Similarly, wear debris was hardly ever noticed in this period.

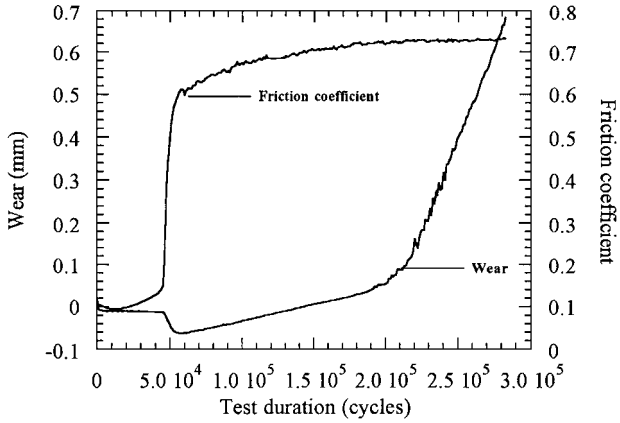

a) Wear and friction of PA 66 running at 0.09 slip ratio, 200 N and 1000 rpm

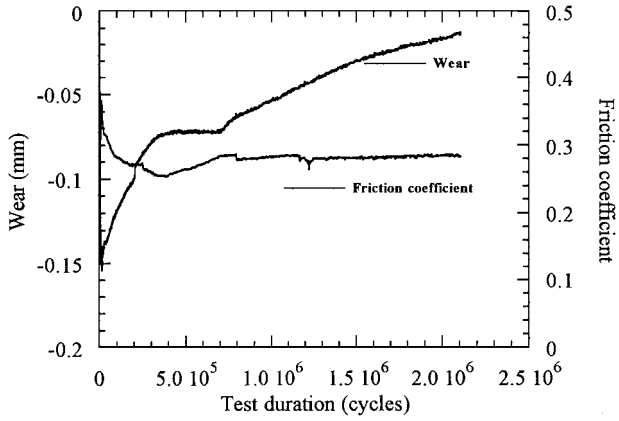

b) Wear and friction of PA 66 running at 0.21 slip ratio, 200 N and 1000 rpm

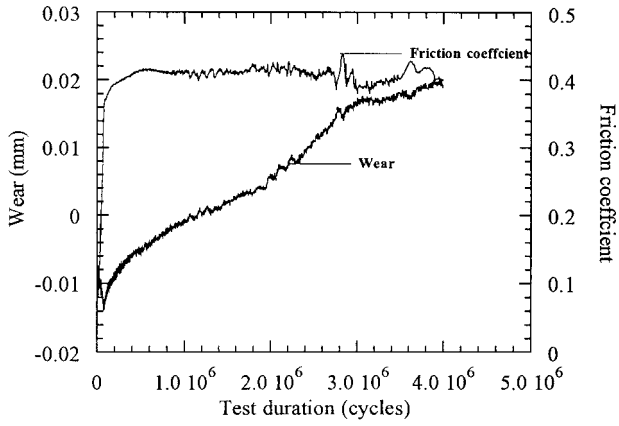

c) At 0.04 slip ratio, 200 N and 1000 rpm

Figure 1 Wear and friction behaviour of PA 66 at different slip ratios.

There is a distinct difference between the wear behaviour as shown in Fig. 1 and that obtained by traditional pin-on-disc tests where it is reported that the wear of PA66 is proportional to time (sliding distance) when it slides in conformal contact [19]. The wear behaviour of PA66 as shown in Fig. 1 is also different from what was reported that the wear was also proportional to sliding distance when PA66 runs against metal in non-conformal contact [20–22].

3.2. Wear rate of unreinforced PA66

Wear rate is defined here as the average depth of material removed from each disc per rolling cycle [14, 18] and was calculated by measuring the weight loss of the specimens. The Hertzian stresses of PA66 discs

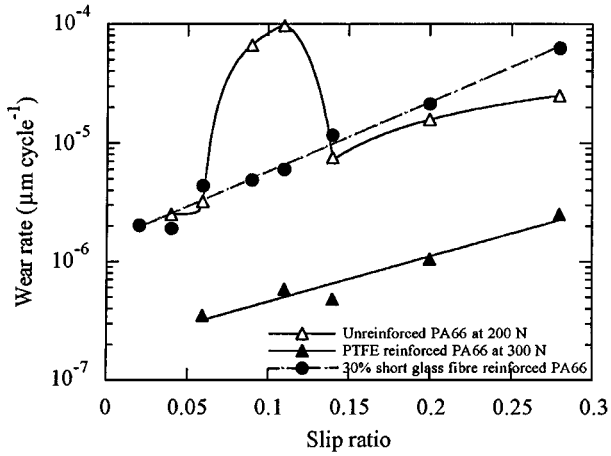

Figure 2 Wear rate vs. slip ratio for PA 66 at 200 N and its composites at 300 N running with 1000 rpm.

and gears were kept identical in order that the test results on discs and gears can be comparable. The contact stress near the pitch line of an unreinforced PA66 gear was 32 MPa, that is equivalent to a normal force of 200 N on a disc. Fig. 2 shows how the wear rate of unreinforced PA66 varies with slip ratio for a fixed normal force of 200 N and a constant running speed of 1000 rpm. It can be seen, as shown in Fig. 2, that slip ratio has a significant effect on the wear rate. The wear rate rises slightly with an increase of slip ratio when the slip ratio is less than 0.09 at which point discoloured material appears on the contact surfaces during these tests. The wear rate starts to increase sharply from 2.0×10^{-6} to 7.0×10^{-5} μm cycle^{-1} as the slip ratio increases from 0.06 to 0.09 and the wear rate reaches its highest value of 10^{-4} μm cycle^{-1} at a slip ratio of 0.11. The unique characteristic property of this material is that a further increase in slip ratio from 0.11 results in a dramatic decrease in wear rate. When the slip ratio increases to 0.14, the wear rate decreases rapidly from 10^{-4} to 8.0×10^{-6} μm cycle^{-1} and discoloured material returns to the contact surfaces. The difference between the two wear rates is over ten times while that between the two slip ratios is approximately 27%. After this considerable decrease, the wear rate increases slowly to 1.0×10^{-5} μm cycle^{-1} as slip ratio increases to 0.21. It is suggested that a slip ratio of 0.11 is a critical one corresponding to maximum wear rate.

Fig. 3 shows effect of normal load on the wear rate of unreinforced PA66 at a given slip ratio and running speed. The wear rate shown in this figure was obtained at 1000 rpm with a slip ratio of 0.04. It can be seen that the wear rate varies in the range from 1.0×10^{-6} to 4.0×10^{-6} μm cycle^{-1}. When the load exceeds 300 N the wear rate starts to increase significantly with load. When the load increases from 300 N to 500 N the wear rate increases from approximately 3.0×10^{-6} to 3.0×10^{-5} μm cycle^{-1}.

3.3. The effect of PTFE and short glass fibres

Results from a limited number of tests of filled PA66 with PTFE show that PTFE has significant effects on

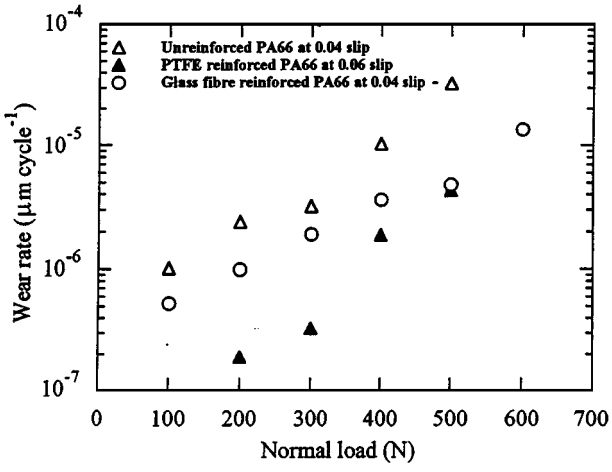

Figure 3 Variation of wear rate with normal load for PA 66 and its composites running at 1000 rpm.

both the wear and friction behaviour of unreinforced PA66 in unlubricated, non-conformal rolling-sliding contact. It was found that the coefficient of friction of the filled PA 66 lay in the range of 0.1–0.12, compared with 0.1–0.3 for PTFE in line contact [23] and with 0.28–0.72 for unreinforced PA66 as shown in Fig. 1.

A comparison of wear rates between the PTFE filled PA66 and unreinforced PA66 is shown in Fig. 2. It can be seen that the wear rate of the filled PA66 with PTFE is ten times lower than that of PA 66 without PTFE. The peak wear rate of unreinforced PA66 seen at a slip ratio of 0.11 disappears almost entirely when it had been filled with PTFE. The effect of PTFE on the wear rate under different loads but with identical slip ratios and running speed is shown in Fig. 3. It can be seen that the filled PA66 with PTFE again reduces the wear rate by approximately ten times at all loads, compared with that of unreinforced PA66.

Reinforcement with short glass fibres also has significant effects on wear and friction. Short glass fibre reinforced PA66 discs were tested with a fixed normal load of 300 N since the contact stress near the pitch line of a short glass fibre reinforced PA66 gear was 63 MPa that is equivalent to 300 N on a composite disc. Both wear and friction are dominated by the ability of a thin film to be formed continuously and to be retained on the surfaces in contact [18]. Similar to the case for unreinforced PA66 at low slip ratios, when the film exists on the contact surface, wear debris could hardly be observed and friction coefficient was less than 0.1. Unlike unreinforced PA66, once the film was disrupted the friction coefficient of short glass-fibre reinforced PA66 varied between 0.25 and 0.3 while that of unreinforced PA66 was in the range of 0.42 to 0.72.

Fig. 3 shows the effect of normal load on the wear rate of 30% short-glass fibre reinforced PA66 composites at a fixed slip ratio of 0.04 and a constant running speed of 1000 rpm. Here, the wear rate increases uniformly on a logarithmic scale from 10^{-7} to 1.35×10^{-5} μm cycle^{-1} as the normal load increases from 100 N to 500 N. Fig. 2 also shows the wear rate of 30% short-glass fibre reinforced PA66 composites as a function of slip ratio for a fixed normal force of 300 N and constant running speed of 1000 rpm. The film on the contact surfaces exists during all these wear-rate measurements. It can be seen that the wear rate increases nearly linearly from 10^{-6} to 10^{-5} μm cycle^{-1} as the slip ratio increases from 0.04 to 0.21. The wear rate is of the same order of magnitude as that of unreinforced PA66, apart from the unique peak in the wear rate.

4. Discussion

4.1. Surface topography

As shown in Fig. 2, the unreinforced PA66 exhibits unique behaviour as a function of wear rate. The wear rate of this material is considerably lower when the slip ratio is either greater or less than the critical slip ratio of 0.11 but shows a peak at 0.11. Therefore, the worn surface was examined at slip ratios around this critical value.

Fig. 4 shows a typical worn surface obtained at a slip ratio of 0.09 on which there is a large amount of a

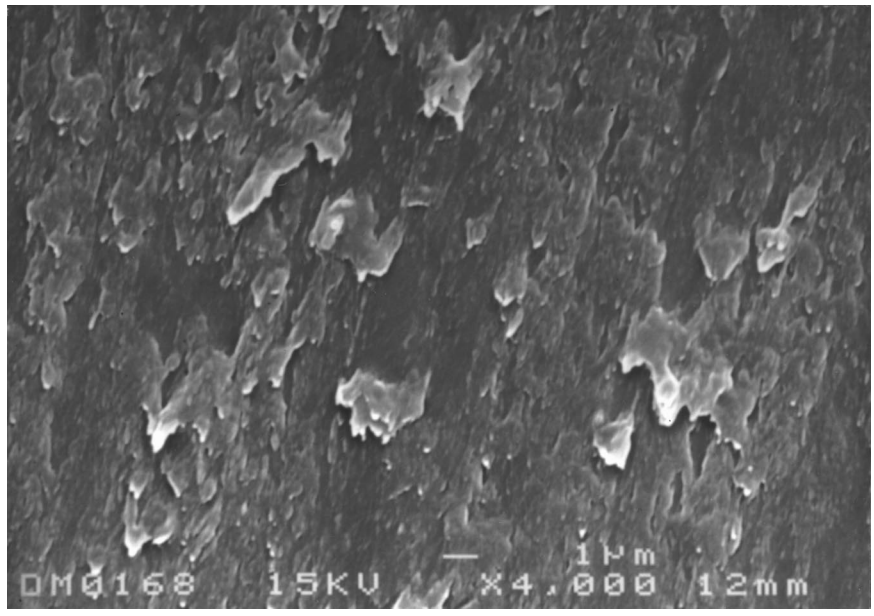

Figure 4 Feature of the PA 66 worn surface running at 0.09 slip ratio, 200 N and 1000 rpm; direction of friction from top to bottom.

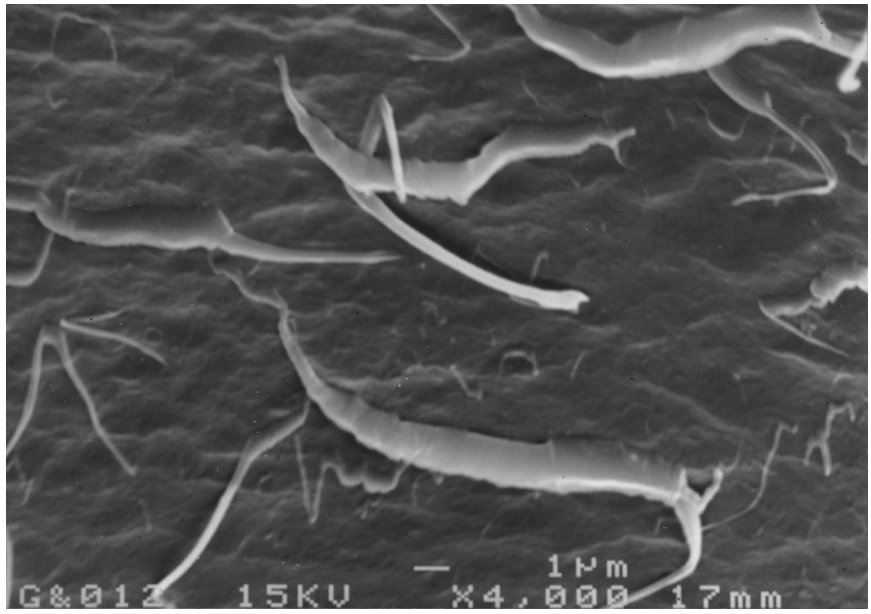

Figure 5 Geometry and dimension of typical debris to be produced on the PA 66 worn surface running at a transition slip ratio of 0.11, 200 N and 1000 rpm; direction of friction from top to bottom.

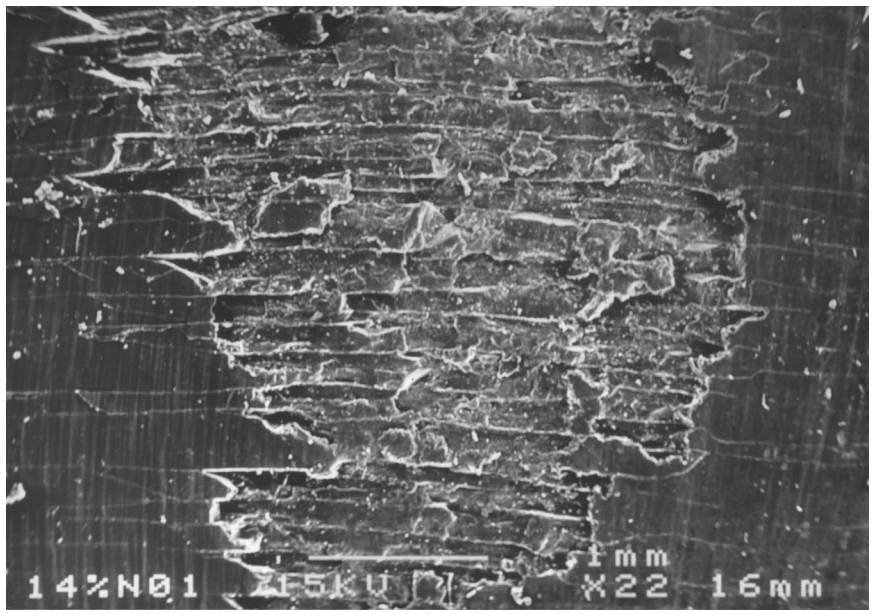

Figure 6 Typical PA 66 worn surface running at 0.14 slip ratio, 200 N and 1000 rpm; direction of friction from bottom to top.

flake-like material. It appeared that there is a layer of film and some flakes on the surface. This film had been sheared strongly during the friction process so that many small flakes started from the film and large pieces of film were pushed in the direction of the friction force. The size of these flakes is from 0.2 to 8.0 μm. Eventually, small flakes grew to 10 μm, then were removed from the contact surface and a piece of debris was formed.

When the slip ratio reached its critical value, that is 0.11, the worn surface shows unique characteristics but is not discoloured. As can be seen in Fig. 5, a large portion of roll-like debris is attached to the surface and accumulates on the surface. It can be seen that roll-like debris consists of the middle part of the roll and two tails on both sides. The length of roll-like debris varies from tens of microns to a couple of hundred microns. The diameter of the middle part is about 1.0–10.0 μm. The tails have a very small diameter (about 0.1 μm) and are very long (about 100 μm). Most of tails were broken and separated from their body during the friction process. It was reported [14] that before roll-like debris on the worn surface was formed, the surface suffered a very deep shear deformation and surface material moved in the direction of friction. This deformed material was gradually rolled in the direction of friction. As a result the body of a piece of roll-like debris was formed, as shown in Fig. 5. It was noted that there was, overall, a great deal of debris collected during the test and that it appeared very thin and long.

Fig. 6 shows a general view of the contact surface after running for 5.8×10^6 cycles after the slip ratio exceeded its critical value. It can be seen that there were many transverse cracks on the worn surface. These cracks occurred along the whole width of the disc and were perpendicular to the direction of the friction force

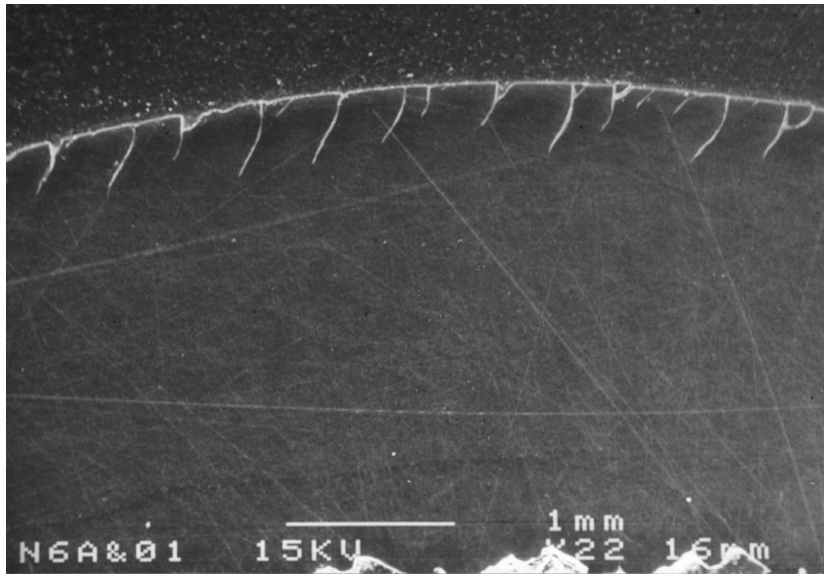

Figure 7 Section through the disc parallel to direction of friction force running at 0.14 slip ratio, 200 N and 1000 rpm; direction of friction from left to right.

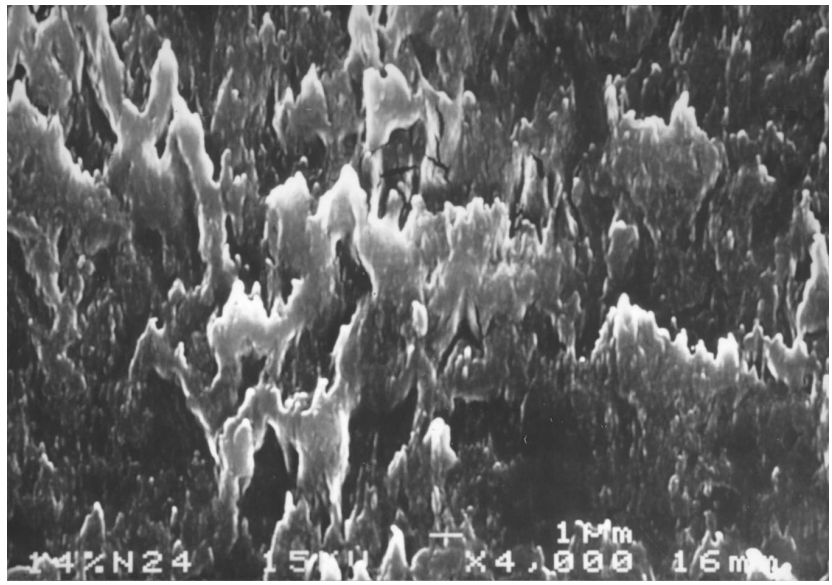

Figure 8 Smeared surface between cracks running at 0.14 slip ratio; 200 N and 1000 rpm; direction of friction from bottom to top.

which is from the bottom to the top in Fig. 6. In the middle of the surface, as shown in Fig. 6, severe spalling can be seen between each pair of cracks and it is suggested that debris collected during the tests was mainly produced in this area. The width between two cracks can be found from Figs 6, 7. Fig. 7 is a section through the disc parallel to the direction of the friction force. It can be seen that the typical width between two fully developed cracks is 200–400 μm and that the distance between two sub-cracks is less than 100 μm. This can be compared with the typical Hertzian contact width of this material, of say 400–980 μm [14]. Some cracks propagated to join their neighbour, and as a result, the material between the two cracks was fractured, severe spalling occurred and debris was formed. It was noted that the crack propagated and fractured gradually rather than suddenly [14].

Fig. 7 also shows the depth of crack propagation. It can be seen that as shown in Fig. 7 the main cracks initiated in the radial direction, perpendicular to the friction force. Then, they propagated in a direction at an angle to the friction force instead of perpendicular to the friction force. The depth to which the main cracks propagated varied from 150 to 450 μm. Between these main cracks there were some sub-cracks. The main cracks propagated up to 450 μm and the small cracks propagated to about a quarter of the depth of the main cracks. These sub-cracks eventually joined the main cracks. As shown in Fig. 7, a sub-crack initiated from the contact surface and propagated in an arc towards the adjacent main crack. Since the sub-crack is wider at the contact surface than beneath it, it is suggested that the small crack was initiated from the contact surface rather than from beneath it [14].

Fig. 8 shows that material on the surface between the cracks was smeared and it appeared that the material had been melted and smeared during the friction process. Compared with the surface film at a slip ratio of

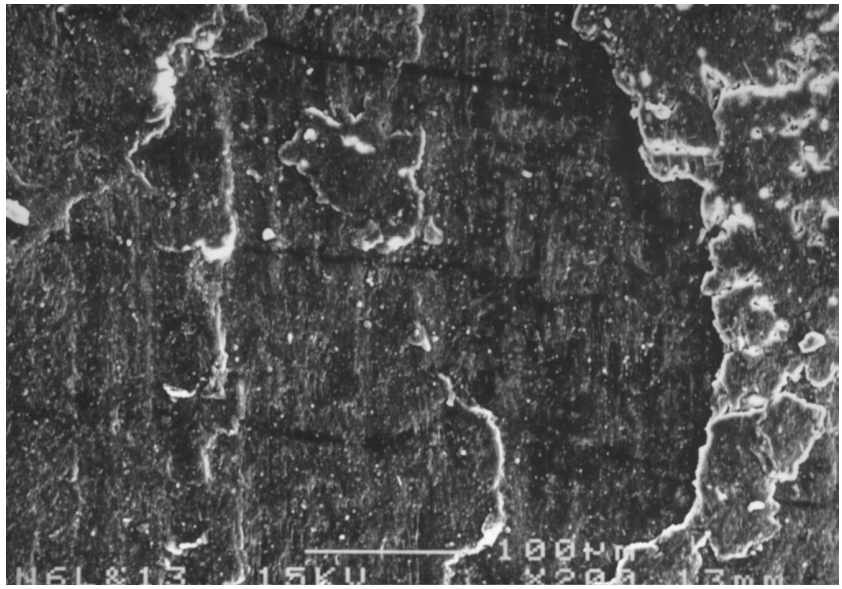

Figure 9 Cracks and surface film on the PA 66 contact surface running at 0.21 slip ratio, 200 N and 1000 rpm; direction of friction from top to bottom.

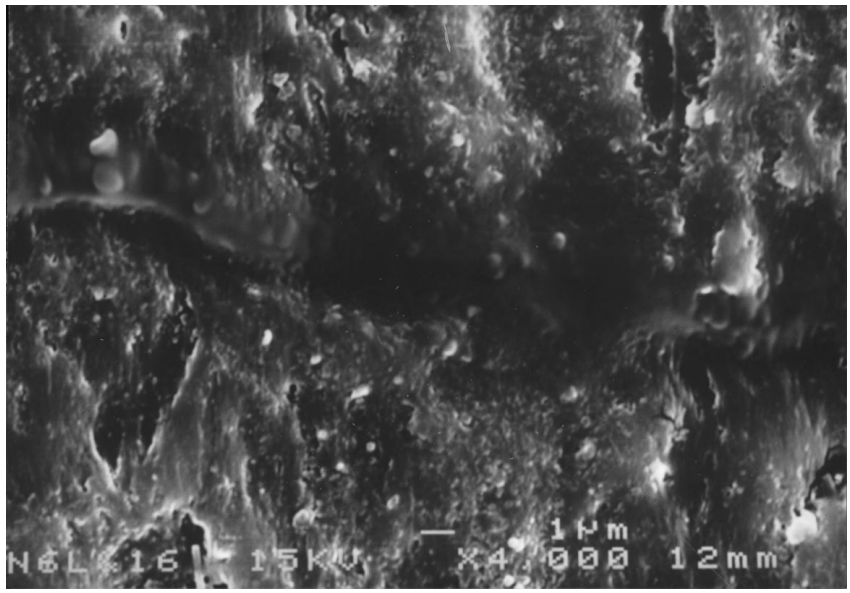

Figure 10 Typical crack covered with film on the contact surface of PA 66 running at 0.21 slip ratio, 200 N and 1000 rpm; direction of friction from top to bottom.

0.09 shown in Fig. 4, the surface material in Fig. 8 was smeared on the whole surface rather than being pulled out separately from the film.

When the slip ratio was increased to 0.21, the worn surface appeared to undergo softening. Fig. 9 shows the surface features on the worn surface after running at a slip ratio of 0.21, 1000 rpm and 200 N. It can be seen that on the worn surface, transverse cracks were covered and a layer of thin material also covered part of the surface. In a similar way to the case of running at 0.14 slip ratio, these cracks propagated to a depth of 200–300 μm and they appeared at about 100–200 μm from each other [14]. Fig. 10 shows the details of one of these covered cracks. It can be seen that the 5 μm wide crack was filled with some material. It is very difficult to believe that the uniform filling as shown in Fig. 10 could have been produced by solid debris. Only very soft material could have done this. Since there was no external lubricant during the test, the material which covered the cracks appears to have come from the material on the contacting surface which was PA66. Therefore it is suggested that the material which covered the crack had been softened and then filled the cracks. Fig.10 shows the flow of surface material of PA66 near the filled crack and it appears that this flow of softened material was due to the very high shear stresses existing when the two discs were in contact.

Also, dark brown discolouration appeared during the tests as well as at higher slip ratios. The worn surface features of PA66 at a lower slip ratio of 0.04 are shown in Figs 11, 12. It can be seen that after 7.2×10^6 cycles transverse cracks perpendicular to the sliding direction were formed. These cracks occurred primarily in the middle of the disc facewidth. The area covered with these cracks varies from 30% to 60% of the whole contact surface, depending on how many cycles the sample has undergone and on the running conditions. Fig. 11 shows the early stage of crack propagation on the worn

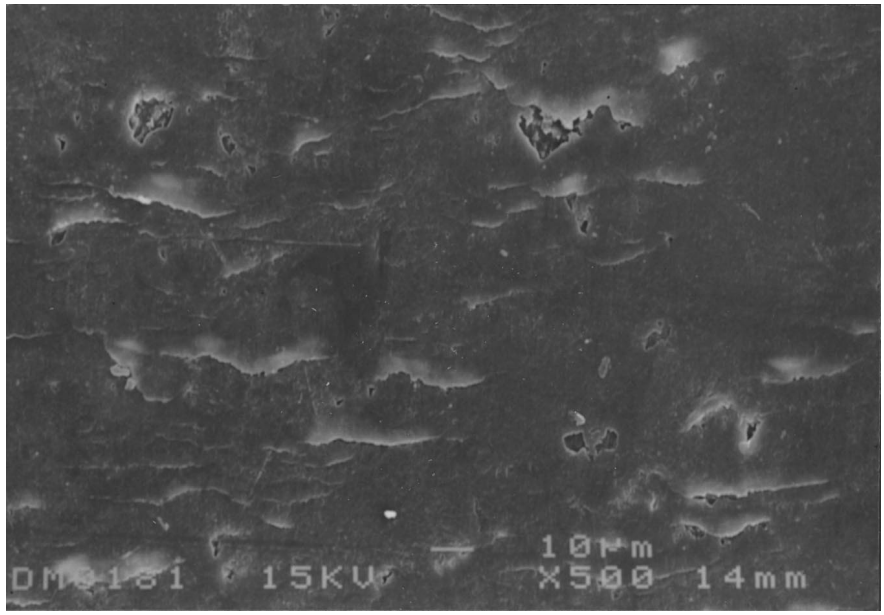

Figure 11 General features of the PA 66 worn surface running at 0.04 slip ratio, 200 N and 1000 rpm; direction of friction from top to bottom.

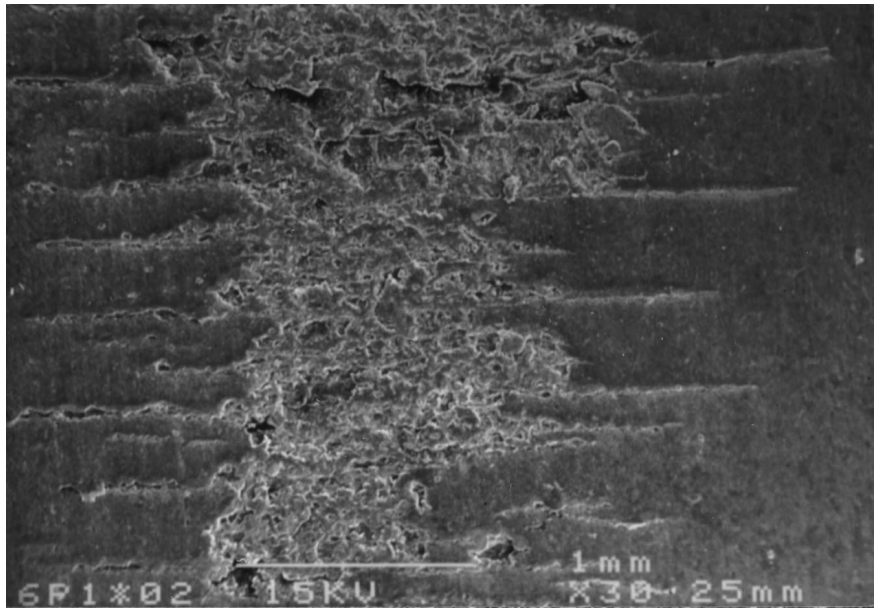

Figure 12 Typical surface features of the PA 66 worn surface running at 0.04 slip ratio, 200 N and 1000 rpm; direction of friction from top to bottom.

surface. It can be seen that the length of these cracks varies from a couple of microns to tens of microns. Fig. 12 shows the area on which cracks have developed fully and this area was located in the middle of the disc facewidth in contact. From this figure, it can be seen that cracks could join together to form a very long crack of several thousands microns. Also, the worn surface between each pair of cracks in the middle area of the contact width has been spalled as a result of these cracks joining. The debris was mainly produced in these areas. The depth that these cracks propagated are very similar to those when PA66 ran at 0.14 slip ratio as shown in Fig. 7.

4.2. Surface temperature characterisation

In an attempt to relate the dramatic change of wear rate and friction coefficient around the critical slip ratio more closely to disc surface temperature an estimate was made of the energy balance between heat generation and dissipation from two discs to obtain a value for the maximum surface temperature of the disc. The heat input to the discs was calculated by using the measured friction coefficient and sliding velocity during tests. The heat loss due to conduction, convection and radiation from the disc surface was estimated [14, 16] to obtain a value for the average disc surface temperature. The flash temperature estimated using Blok's equation was then superimposed. Details are given in the Appendix. The result is thought to be accurate to within about 15% of the rise above ambient temperature and thus to around $\pm 30^{\circ}$C at the highest generated temperatures. Fig. 13 shows the results for unreinforced and PTFE filled PA66 from the estimate of the maximum surface temperature of the disc during the wear process. As shown in Fig. 13, it can be seen that the maximum surface temperature of unreinforced

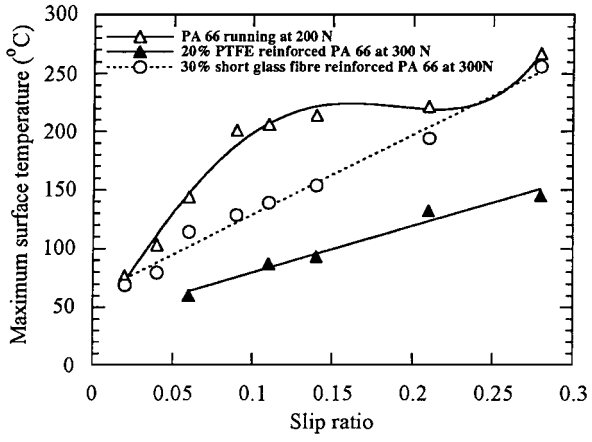

Figure 13 Maximum surface temperature vs. slip ratio of PA 66 and its composites running at 1000 rpm.

PA66 increases steeply up to the critical slip ratio of 0.11 at which it is 206°C, then increases more slowly.

Surface temperature monitoring with the infra-red camera has revealed an important phenomenon for unreinforced PA66. It was observed that when the slip ratio was less than the critical slip ratio of 0.11, the measured surface temperature [16, 24] was nearly constant during the wear process. However, once the slip ratio exceeded 0.11 it was found that within the first couple of million cycles the measured surface temperature decreased with the number of cycles during the friction process. After the temperature reached 255°C as shown in Fig. 1 it started to decrease gradually with the number of cycles and was reduced to 221°C and remained constant until the end of the test. In the meantime, the measured friction force exhibited some decrease. When the slip ratio was 0.14, the measured temperature showed similar behaviour to that at the slip ratio of 0.21. It reached 248°C at first then decreased steadily and eventually remained at about 214°C. The measured friction showed a similar drop. Eventually, the temperature was about 214°C–221°C when the slip ratio was in the range from 0.14 to 0.21.

4.3. Function and formation of the thin film

The physical observations during the tests suggest that the low wear rates shown in Fig. 2 are always correlated with dark brown coloured and more polished material on the contact surfaces. By contrast, the phenomenon of the brown and polished surface during tests never occurs near the peak wear rate at the critical slip ratio of 0.11. It is suggested that this surface feature was related to a layer of thin film on the contact surfaces as observed by surface characterisation with SEM, as shown Figs 8–10. It appeared that the dramatic change of the wear rate around 0.09–0.11 slip ratio was correlated with unformed film, as shown in Fig. 5, and that the low value regions of the wear rates shown in Fig. 2 corresponded to the appearance of the thin film, as shown in Figs 8–10. The function of the thin film on the worn surfaces appeared to decrease the friction between both contact surfaces significantly and subsequently kept the wear rate low. With this film on the surface, little wear debris can be found. The wear rate determined by weighing is around 10^{-6} μm cycle^{-1} and increases gradually with slip ratio. The friction coefficient varies from 0.28 to 0.42. This property of the unreinforced PA66 here is similar to that of the transfer film reported when the unreinforced PA66 runs against metals [25, 26].

The thin film on the contact surfaces was discoloured significantly after tests, thus indicating surface degradation. This might suggest that the contact at a high slip ratio took place with effectively a layer of liquid polyamide lubricant. As shown in Fig. 13, the maximum surface temperature increased from 206 to 221°C when the slip ratio exceeded its critical value of 0.11 and rose to 0.21. These high surface temperatures are very close to the melting point of 255°C for unreinforced PA66 and agree well with the suggestion of a layer of liquid polyamide. However, under conditions of low load and slip ratio the thin film is also discoloured and so the degradation is unlikely to be due simply to melting of the polyamide. The maximum surface temperature confirms this suggestion because the temperature was lower than 144°C at slip ratios less than 0.06 and was far from its melting point. The extent of the colour change varies with the number of contact cycles, and it appeared that repeated contact between the thin films may lead to surface degradation. This requires further investigation.

When the slip ratio was at its critical value of 0.11, the maximum surface temperature on the worn surface was approximately 206°C. There was no film on the contact surface during tests. Instead, a great deal of roll debris formed, as shown in Fig. 5. It is suggested that over a range of surface temperature, material on the contact surface is not smeared to form a thin film but forms rolls during the friction process. Without the protection of the thin film on the contact surface, the friction coefficient is very high and is in the range from 0.62 to 0.72. These rolls are not able to stay on the contact surface, and as a result, there is a great amount of roll debris found and collected during the tests and the wear rates are extremely high.

Therefore, it appears that the maximum surface temperature dominates the formation of the thin film on the contact surface, and subsequently plays a very important role in controlling the wear rate for unlubricated, rolling-sliding contact. A range of surface temperature around 206°C should be avoided to achieve low wear rates.

4.4. Mechanism for transverse cracks

The second unique property of unreinforced PA66 is the existence of many transverse cracks perpendicular to the direction of the friction force on the worn surface when the slip ratios are not near the critical slip ratio. As described in the surface topography characterisation, these cracks initiated on the contact surface of the disc. A numerical analysis of the contact mechanism suggested that the maximum shear stress should appear on the contact surface rather than on the subsurface since the friction coefficient of unreinforced PA66 is greater than 0.25 [27]. Therefore, when two discs

are in rolling-sliding contact, large shear strain can be accumulated on the contact surface. As a result, the cracks are initiated on the contact surface rather than in the subsurface as classical theory suggests. Surface characterization agrees well with this suggestion [14]. However, once a crack has formed it appears to reduce the surface tensile stress in its vicinity and to inhibit the formation of further cracks. As the cracks penetrate into the disc the magnitude of the tensile stresses at the crack tip would appear to fall and crack propagation may cease. As shown in Fig. 7, it was noted that the depth of these cracks varied around several hundreds of microns but never exceeded 500 μm.

Crack initiation on the surface may also be due to PA66 being semi-crystalline. The crystallinity of disc material was measured by differential scanning calorimetry (DSC) and is 33%. When PA66 discs are in rolling-sliding contact, the maximum surface temperature varies with running conditions. Even at a slip ratio of 0.04, 200 N and 1000 rpm the maximum surface temperature is about 100°C, as shown in Fig. 13. This temperature is much higher than the glass transition of 50°C. Therefore the amorphous phase of PA66 on the contact surface may become rubbery, i.e. the surface material may behave as a rubber. In fact, the worn surface features as shown in Fig. 11 are similar to the typical failure pattern of a rubber surface except for the dimensions and distribution of cracks [28, 29]. It is suggested that when two semi-crystalline PA 66 discs are in rolling-sliding contact some tears were generated at the rear of the contact region and that the tears were almost normal to the direction of sliding. A raised lip is teased out of the contact surface but no removal of material occurs. It appears that the tearing at the rear of contact area may be due to the tensile stress from the friction process which can be great enough to rupture the material as with rubber.

The crack from the raised lip as shown in Fig. 11 can be fully propagated if the number of stress cycles in contact is great enough. As shown in Fig. 12, when the cracks have propagated fully, joined each other and spread over the whole contact surface, the surface became rougher and lump-like debris spalled off. Then at a later stage wear becomes severe which should correspond to the third wear phase shown in Fig. 1. It was noted during the tests that production of debris always occurred when the cracks were developed fully. Therefore, it is suggested that the wear rate is not directly correlated with the growth rate of fatigue cracks as the classical theories suggest. Such phenomenon appears to be similar to that reported by Clerico [20–22].

The crack propagation is also related to the contact stress. The surface shown in Fig. 12 resulted from the central area in contact where it is more difficult for heat to be dissipated so that more thermal expansion occurred. As a result, the central area in contact suffered from higher contact stress than the area near the edge of the facewidth in contact where it is easy for the surface heat to be dissipated. It was observed by an infra-red camera that during tests, the surface temperature in the central area was about 15°C higher than that of the area near the edge of facewidth. This suggests that the higher the contact stress and the greater the temperature, the faster the cracks propagated.

4.5. The effect of PTFE filler and short-glass fibre reinforcement on transverse cracks

Transverse cracks on the contact surfaces up to 450 μm depth in unreinforced PA66 are a serious disadvantage if the material is used in engineering components, such as gears. To suppress them on the contact surface, PTFE filled PA66 was tested under the same slip ratios and running speeds as unreinforced PA66. The applied load was 300 N. It was noted that no macro-transverse cracks on the worn surfaces were observed with a variety of slip ratios. A typical surface topography is shown in Fig. 14, which was obtained after six million cycles under 0.11 slip ratio, 300 N and 1000 rpm. It can be

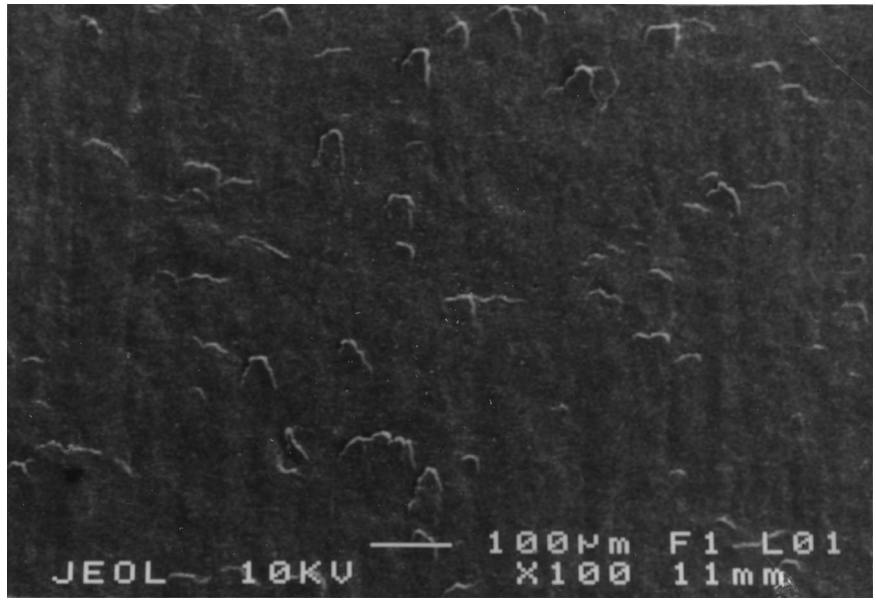

Figure 14 Typical PTFE reinforced PA 66 worn surface running at 0.11 slip ratio, 300 N and 1000 rpm; direction of friction from top to bottom.

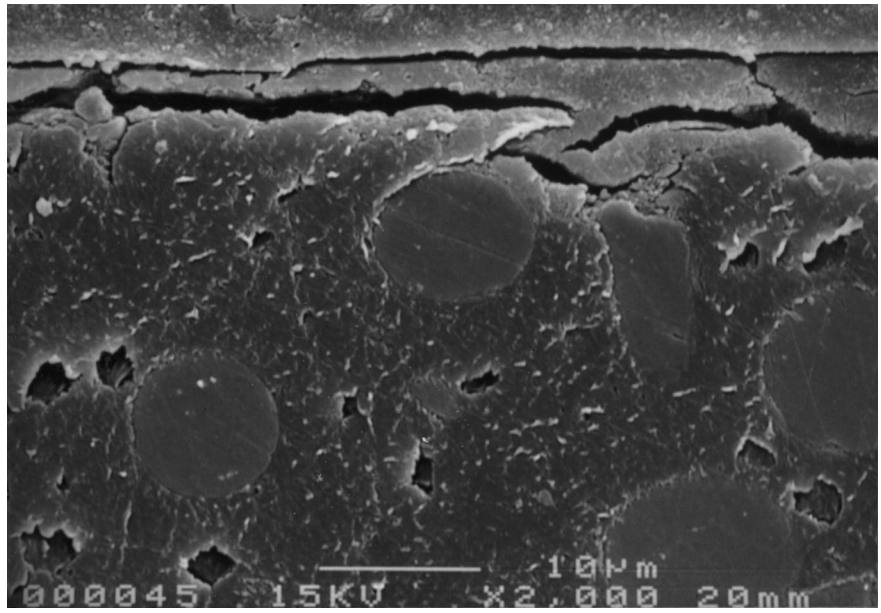

Figure 15 Section through a typical surface film on the contact surface of short glass fibre reinforced PA66 running at 1000 rpm, 0.04 slip ratio and 300 N; direction of friction from left to right.

seen that transverse cracks in unreinforced PA66 on the contact surface shown in Figs 6, 7, 9, 12 disappear completely on the PTFE filled PA66 worn surface. Instead, there are many small flakes on the contact surface and they remained in the range of 100 μm as shown in Fig. 14. Therefore, it is suggested that once PA66 is filled with PTFE, macro-transverse cracks can effectively be suppressed.

The effect of PTFE filler on macro-transverse cracks is to suppress both initiation and propagation of transverse cracks on the contact surface. As described in the last section, since the coefficient of friction of the filled PA66 with PTFE was around 0.12 and much smaller than critical value of 0.25 when two unreinforced PA66 discs were in contact, the maximum shear stress should appear on the subsurface rather than on the contact surface. It appears that small flakes on the surface as shown in Fig. 14 are not initiated from the contacting surface. Therefore, it is suggested that when two discs were in rolling-sliding contact, crack initiation of PTFE filled PA66 should appear in the subsurface as classical theory suggests. This suggestion agrees well with the surface topography shown in Fig. 14. Subsequently, no transverse cracks appear on the contact surface.

The reinforcement with short-glass fibre of PA66 also has an effect on transverse cracks which occur when unreinforced PA66 is in non-conformal rolling-sliding contact as shown in Figs 6, 7, 9, 12. Although the wear mechanisms are very complicated [18], as shown in Fig. 15, no transverse cracks on the worn surfaces were observed under a variety of test conditions. Because of the film on the surface [18], the friction coefficient can be below 0.1, and as a result, the shear stress at the interface between the films should be low. This low shear stress may play an important role in the low friction coefficient, therefore, the maximum shear stress is not at the contact surface but in the subsurface and there is little chance for a transverse crack to initiate on the contact surface.

5. Application to PA 66 gears

The properties of unreinforced PA66 which have been investigated may be applied to solve some engineering problems for polyamide gears. A typical question in gearing of polyamide is why PA66 gear teeth fracture near the pitch line area with little debris where the sliding ratio between gear teeth in mesh is very small [6, 7, 11, 12].

From the above study of non-conformal unlubricated rolling-sliding contact, one of the dominating factors in surface failure at low and high slip ratios is transverse crack propagation on the surfaces in contact. Also there was not much debris before cracks fully developed and spalled. Assuming that the slip ratio on the gears teeth in contact varies from 0 to 0.21 [6, 7, 11, 12], the behaviour of crack propagation on a gear tooth surface should be similar to that on disc surfaces. In other words, these cracks on a gear tooth propagate not only towards the gear facewidth but also downwards to the subsurface of the gear tooth. After a certain number of cycles, the cracks will propagate down to a depth of 0.5 mm near the dedendum of a gear tooth where a high slip ratio is expected and near the pitch line area on the gear tooth where a low slip ratio occurs. For a gear of module 2 mm, the thickness of a gear tooth on the dedendum is about 2.5 mm and that on the pitch line is 2 mm [7, 8]. Thus the bending stress on the dedendum of the tooth could be much higher than it was designed for due to both significant decreases of the thickness of the gear tooth and severe stress concentrations at the tip of cracks. Near the pitch line area on a gear tooth, corresponding to lower slip ratios, bending stresses are high since this is the position of lowest contact ratio. Crack propagation at lower slip ratios also will cause severe stress concentrations at the tip of cracks if the tooth is subjected to a reasonable higher bending moment. Under high bending stresses, it is possible that the severe stress concentration results in the tooth fracture near the pitch line area on the gear

tooth. Therefore it is suggested that tooth fracture in PA66 gears is due to initiation and propagation of transverse cracks rather than creep. In fact, the cracks on a PA66 gear tooth surface before the gear tooth fractured have been observed [30] and this evidence supports the suggestion.

6. Conclusions

1. The wear and friction of unreinforced polyamide66 running against itself in unlubricated rolling-sliding contact has been investigated under a wide range of slip ratios and loads. It was found that slip ratio has a significant effect on the wear rate. There are three major features of the unreinforced PA66: a critical slip ratio under certain load and running speed, macro-transverse cracks and a layer of film on the contact surface.

2. At the critical slip ratio at a fixed load and running speed, the unreinforced PA66 shows very poor wear resistance and high friction coefficient. The wear rate has a rather steep increase from 10^{-6} μm cycle^{-1} up to 10^{-4} μm cycle^{-1}. The friction coefficient increases sharply from 0.42 up to 0.72. When the slip ratio approached the critical ratio, material on the surface was sheared strongly during the friction process so that many small flakes formed from the film and large pieces of film were pushed in the direction of the friction force. Further increases of the slip ratio up to 0.11 resulted in severely deformed material flow on the contact surface. This material flows and was, gradually, rolled in the direction of friction. A large portion of roll-like debris was attached to the surface, which corresponds to very high wear rate of 10^{-4} μm cycle^{-1}. This phenomenon was related to the surface temperature at a given load and speed at which the material could form rolls from the worn surface. A range of surface temperature around 206°C should be avoided if a low wear rate is expected.

3. Beyond the critical slip ratio, the unreinforced polyamide 66 has high wear resistance which is dominated by material softening and film formation on the contact surfaces. A layer of thin film results from softened material on the surface corresponding to a low friction coefficient and behaves as a self-lubrication layer. The wear rate varies with slip ratio in the range of 2.0–8.0 $\times 10^{-4}$ μm cycle^{-1} and the friction coefficient decreases with an increase of slip ratio and varies from 0.28 to 0.42. A gradual decrease of surface temperature from near the melting point and surface characterisation give further evidence of the self-lubricating property of unreinforced PA66.

4. Many macro-transverse cracks in the unreinforced PA66 on the contact surfaces are a serious disadvantage if the material is applied in engineering components. These transverse cracks are perpendicular to the direction of the friction force on the worn surface, are initiated on the contact surface, propagate in the direction of facewidth and penetrate to a depth of 150–450 μm. It appears that crack initiation and propagation on the material surface are dependent on a high friction coefficient (above 0.25), a semi-crystalline structure, contact stresses, surface temperature and number of contact cycles.

5. Some of the tribological properties of unreinforced PA66 from disc tests presented in this paper correspond closely to those in PA66 gears. Both had transverse cracks when they ran against each other and both ran smoothly without much debris before cracks fully developed and spalled. It appears to be the transverse cracks that cause unreinforced PA 66 gear teeth to fracture even near the pitch line where the sliding ratio between gear teeth in mesh is very low.

6. The filler of PTFE has a significant effect on transverse cracks on the contact surfaces of PA66. This filled PA66 suppresses both initiation and propagation of transverse cracks that occurred in unreinforced PA66 and decreases both the wear rate and the friction coefficient fairly considerably. The short-glass fibre reinforced PA66 composite prevents also transverse cracks from both initiation and propagation. A thin film layer on the contact surfaces plays a dominant role both in reducing wear and friction and in suppressing transverse cracks when two composite discs run against each other.

Appendix: Calculation of maximum surface temperature

A.1. Bulk temperature T_b

The energy input Q can be given by

$$Q = \mu F_n |V_1 - V_2| \tag{A1}$$

where V_1 and V_2 are the rolling speeds of two discs respectively, μ the friction coefficient and F_n the normal load applied to the discs.

The energy loss due to convective heat dissipation Q_1 may be expressed as [31]

$$Q_1 = 0.664 b k_a (T_b - T_a) \sqrt[3]{\frac{\eta_a c_p}{k_a}} \sqrt{\frac{\nu_r L_d}{\nu}} \tag{A2}$$

where b is the disc facewidth; k_a the thermal conductivity of air (=0.025 W m^{-1} K^{-1}); η_a the dynamic viscosity of air (=2 $\times 10^{-5}$ kg m^{-1} s^{-1}); c_p the specific heat capacity of air (=1 kJ kg^{-1} K); ν_r the air velocity relative to disc, which is equal to the rolling speed of the disc; ν the kinematic viscosity of air (=1.9 $\times 10^{-5}$ m^2 s^{-1}); L_d the circumference of the disc; T_a the free air temperature (ambient temperature) measured during the tests; T_b the body temperature of the disc surface in contact.

The energy loss due to conductive heat dissipation Q_2 may be given by [32]

$$Q_2 = \frac{2\pi b k_p}{\ln\left(\frac{r_o}{r_i}\right)} (T_b - T_i) \tag{A3}$$

where r_o is the outside radius of the disc, r_i its inner radius and T_i the temperature on the inner ring surface of the disc. T_i was taken as being equal to the temperature of the shaft on which disc is mounded tightly.

For the radiation component, the energy Q_3 dissipated due to radiation from each disc can be given as follows [33]

$$Q_3 = \sigma A_d \varepsilon_{rad} \left(T_b^4 - T_a^4\right) \tag{A4}$$

where σ is Stefan-Boltzmann constant ($=5.669 \times 10^{-8}\,\mathrm{W\,m^{-2}\,K^{-1}}$), $\varepsilon_{\mathrm{rad}}$ the emissivity of the disc material and A_{d} the effective area of disc surface dissipating radiation energy.

For the whole system consisting of two discs in contact, if the temperature on the contact surfaces is stable, an energy balance may be assumed. Therefore, the heat generation in the system should be equal to the heat dissipation in it and can be expressed as

$$Q = \mu F_{\mathrm{n}} |V_1 - V_2| = (Q_1 + Q_2 + Q_3)_{\mathrm{t}} + (Q_1 + Q_2 + Q_3)_{\mathrm{b}} \tag{A5}$$

where t is the top and b is the bottom disc. The average bulk surface temperature T_{b} can be obtained by a simple numerical calculation.

A.2. Flash temperature T_{f}

The classic model of the flash temperature from Blok [34] is employed and can be given

$$T_{\mathrm{f}} = \frac{1.11 \mu F_{\mathrm{n}} \left| \sqrt{V_1} - \sqrt{V_2} \right|}{b \sqrt{k \rho c w}} \tag{A6}$$

where ρ is the density of the disc materials, c the specific heat capacity of the disc materials and w the Hertzian contact width.

A.3. Maximum contact surface temperature

The total maximum surface temperature T_{max} was obtained by superimposing the bulk tempearture and flash temperature as follow:

$$T_{\mathrm{max}} = T_{\mathrm{b}} + T_{\mathrm{f}}. \tag{A7}$$

Acknowledgement

We would like to thank the Davall Gear Company and Davall Moulded Gears Ltd for their continued interest in, and support of, this work.

References

1. K. FRIEDRICH, "Advances in Composite Tribology" (Elsevier, London, 1993) p. 109.
2. L. A. CARLSSON, "Thermoplastic Composite Materials" (Elsevier, Oxford, 1991) p. 103.
3. LNP Engineering Plastics Inc, "A Guide to LNP's Internal Lubricated Thermoplastics" (LNP, USA, 1994) pp. 1–10.
4. M. J. FOLKES, "Short Fibre Reinforced Thermoplastics" (Wiley, Chichester, 1982) p. 1.
5. H. VOSS and K. FRIEDRICH, *Wear* **116** (1987) 1.
6. G. CRIPPA and P. DAVOLI, *Kunststoffe* **81** (1991) 147.
7. K. MAO, C. J. HOOKE and D. WALTON, *J. Synth. Lubr.* **4** (1995) 337.
8. British Standard BS 6168, "Specification for Non-metallic Spur Gears" (British Standards Institution, London, 1987).
9. "Polypenco Gear Design" (Polypenco Corporation, USA, 1985) p. 32.
10. R. J. DRAGO, "Fundamentals of Gear Design" (Butterworths, Boston, 1988) p. 211.
11. C. J. HOOKE, K. MAO, D. WALTON, A. R. BREEDS and S. N. KUKUREKA, *ASME Journal of Tribology* **115** (1993) 119.
12. G. CRUPPA, in Proceedings of the 4th World Congress on Gearing and Power Transmission, (MCI, Paris, 1999) Vol. 1 p. 761.
13. Y. YAMAGUCHI, "Tribology of Plastic Materials" (Elsevier, New York, 1990) p. 326.
14. Y. K. CHEN, PhD dissertation, The University of Birmingham, Birmingham, 1996.
15. S. N. KUKUREKA, Y. K. CHEN, C. J. HOOKE and P. LIAO, in Proceedings of the 1994 International Gearing Conference, Newcastle, September 1994, edited by J. N. Fawcett (Mechanical Engineering Publications Limited, London, 1994) p. 14.
16. *Idem., Wear* **185** (1995) 1.
17. P. J. GUICHEAAR, B. S. LEVY and N. M. PARIKH, "Gear Manufacture and Performance" (American Society for Metals, Ohio, USA, 1974) p. 83.
18. Y. K. CHEN, S. N. KUKUREKA and C. J. HOOKE, *Journal of Materials Science* **31** (1996) 5643.
19. K. FURBER, J. R. ATKINSON and Dowson, in Proceedings of the 3rd Leeds-Lyon Symposium on Tribology (MEP, London, 1978) p. 25.
20. M. CLERICO, *Wear* **13** (1969) 183.
21. *Idem., ibid.* **64** (1980) 259.
22. M. CLERICO and V. PATIERNO, *ibid.* **53** (1979) 279.
23. C. POOLEY and D. TABOR, *Proceedings of Royal Society*, **A329** (1972) 251–274.
24. C. J. HOOKE, S. N. KUKUREKA, P. LIAO, M. RAO and Y. K. CHEN, *Wear* **197** (1996) 115.
25. K. TANAKA, *ASME Journal of Lubrication Technology* **99** (1977) 408.
26. J. H. BYETT and C. ALLEN, *Tribology International* **25** (1992) 237.
27. M. RAO, PhD dissertation, The University of Birmingham, Birmingham, 1997.
28. B. J. BRISCOE and D. TABOR, in Proc. Int. Conf. on the Fundamentals of Tribology (MIT Press, Massachusetts, USA, 1978) p. 733.
29. Y. FUKAHORI and H. YAMAZAKI, *Wear* **171** (1994) 195.
30. N. WRIGHT, MPhil dissertation, The University of Birmingham, Birmingham, 1996.
31. A. D. YOUNG, "Boundary Layers" (Blackwell, Oxford, 1989).
32. J. R. SIMONSON, "Engineering Heat Transfer" (Macmillan, London, 1975).
33. J. P. HOLMAN, "Heat Transfer" (McGraw-Hill, London, 1992).
34. H. BLOK, *Wear* **6** (1963) 483.

Received 13 January 1998
and accepted 22 July 1999